

# Self-Supervised Learning for Medical Image Classification: A Systematic Review and Implementation Guidelines

*Shih-Cheng Huang<sup>1,2\*</sup>, Anuj Pareek<sup>1,2\*</sup>, Malte Jensen<sup>1</sup>, Matthew P. Lungren<sup>1,2,3</sup>, Serena Yeung<sup>1,2,4,5,6‡</sup>, Akshay S. Chaudhari<sup>1,2,3,7‡</sup>*

<sup>1</sup> Department of Biomedical Data Science, Stanford University, Stanford, CA, USA

<sup>2</sup> Center for Artificial Intelligence in Medicine & Imaging, Stanford University, Stanford, CA, USA

<sup>3</sup> Department of Radiology, Stanford University, Stanford, CA, USA

<sup>4</sup> Department of Computer Science, Stanford University, Stanford, CA, USA

<sup>5</sup> Department of Electrical Engineering, Stanford University, Stanford, CA, USA

<sup>6</sup> Clinical Excellence Research Center, Stanford University School of Medicine, Stanford, CA, USA

<sup>7</sup> Stanford Cardiovascular Institute, Stanford University, CA, USA

{\*,‡} Equal Contribution

## Abstract

Advancements in deep learning and computer vision provide promising solutions for medical image analysis, potentially improving healthcare and patient outcomes. However, the prevailing paradigm of training deep learning models requires large quantities of labeled training data, which is both time-consuming and cost-prohibitive to curate for medical images. Self-supervised learning (SSL) has the potential to make significant contributions to the development of robust medical imaging models through its ability to learn useful insights from copious medical datasets without labels. In this review, we provide consistent descriptions of different self-supervised learning strategies and compose a systematic review of papers published between 2012 and 2022 on PubMed, Scopus, and ArXiv that applied self-supervised learning to medical imaging classification. We screened a total of 412 relevant studies and included 79 papers for data extraction and analysis. With this comprehensive effort, we synthesize the collective knowledge of prior work and provide implementation guidelines for future researchers interested in applying self-supervised learning to their development of medical imaging classification models.

## Main

The utilization of medical imaging technologies has become an essential part of modern medicine, enabling diagnostic decisions and treatment planning. The importance of medical imaging is exemplified by the consistent rate of growth in medical imaging utilization in modern healthcare<sup>1,2</sup>. However, as the number of medical imaging relative to the available radiologists continues to become more disproportionate, the workload for radiologists continues to increase. Studies have shown that an average radiologist now needs to interpret one image every 3-4 seconds to keep up with clinical workloads<sup>3-5</sup>. With such a huge cognitive burden placed on radiologists, delays in diagnosis and diagnostic errors are unavoidable<sup>6,7</sup>. Thus, there is an urgent need to integrate automated systems into the medical imaging workflow, which will improve both efficiency and accuracy of diagnosis.

In recent years, deep learning models have demonstrated diagnostic accuracy comparable to that of human experts in narrow clinical tasks for several medical domains and imaging modalities, including chest and extremity X-rays<sup>8-10</sup>, computed tomography (CT)<sup>11</sup>, magnetic resonance imaging (MRI)<sup>12</sup>, whole slide images (WSI)<sup>13,14</sup>, and dermatology images<sup>15</sup>. While deep learning provides promising solutions for improving medical image interpretation, the current success has been largely dominated by supervised learning frameworks, which typically require large-scale labeled datasets to achieve high performance. However, annotating medical imaging datasets requires domain expertise, making large-scale annotations cost-prohibitive and time-consuming, which fundamentally limits building effective medical imaging models across varying clinical use cases.

Besides facing challenges with training data, most medical imaging models underperform in generalizing to external institutions or in attempting to repurpose for other tasks<sup>16</sup>. The inability to generalize can be largely due to the process of supervised learning, which encourages the model to mainly learn features heavily correlated with specific labels rather than general features representative of the whole data distribution. This creates specialist models that can perform well only on the tasks they were trained to do<sup>17</sup>. In a healthcare system where myriad opportunities and possibilities for automation exist, it is practically impossible to curate labeled datasets for all tasks, modalities, and outcomes for training supervised models. Therefore, it is important to develop strategies for training medical AI models that can be fine-tuned for many downstream tasks, while remaining pragmatic regarding the challenges in curating large-scale labeled datasets.

Self-supervised learning (SSL), the process of training models to produce meaningful representations using unlabeled data, is a promising solution to challenges caused by difficulties in curating large-scale annotations. Unlike supervised learning, self-supervised learning can create generalist models that can be finetuned for many downstream tasks without large-scale labeled datasets. Self-supervised learning was first popularized in the field of natural language processing (NLP), when researchers leveraged copious amounts of unlabeled text scraped from the internet to improve the performance of their models. These pretrained large language models<sup>18,19</sup>, are capable of achieving state-of-the-art results for a wide range of NLP tasks, and have shown the ability to perform well on new tasks with only a fraction of the labeled data that traditional supervised learning techniques require. Motivated by the initial success of SSL in NLP, there is great interest in translating similar techniques of SSL to computer vision tasks. Such work in computer vision has already demonstrated performance for natural images that is superior to that achieved by supervised models, especially in label-scarce scenarios<sup>20</sup>.

Reducing the number of manual annotations required to train medical imaging models will significantly reduce both the cost and time required for model development, making automated systems more accessible to different specialties and hospitals, thereby reducing workload for radiologists and potentially improving patient care. While there is already a growing trend in recent medical imaging AI literature to leverage self-supervised learning (Figure 1), as well as a few narrative reviews<sup>21,22</sup>, the most suitable strategies and best practices for medical images have not been sufficiently investigated. The purpose of this work is to present a comprehensive review of deep learning models that leverage self-supervised learning for medical image classification, define and consolidate relevant terminology, and summarize the results from state-of-the-art models in relevant current literature. We focus on medical image classification tasks because many clinical

tasks are based on classification, and thus our research may be directly applicable to deep learning models for clinical workflows. This review intends to help inform future modeling frameworks and serve as a reference for researchers interested in the application of self-supervised learning in medical imaging.

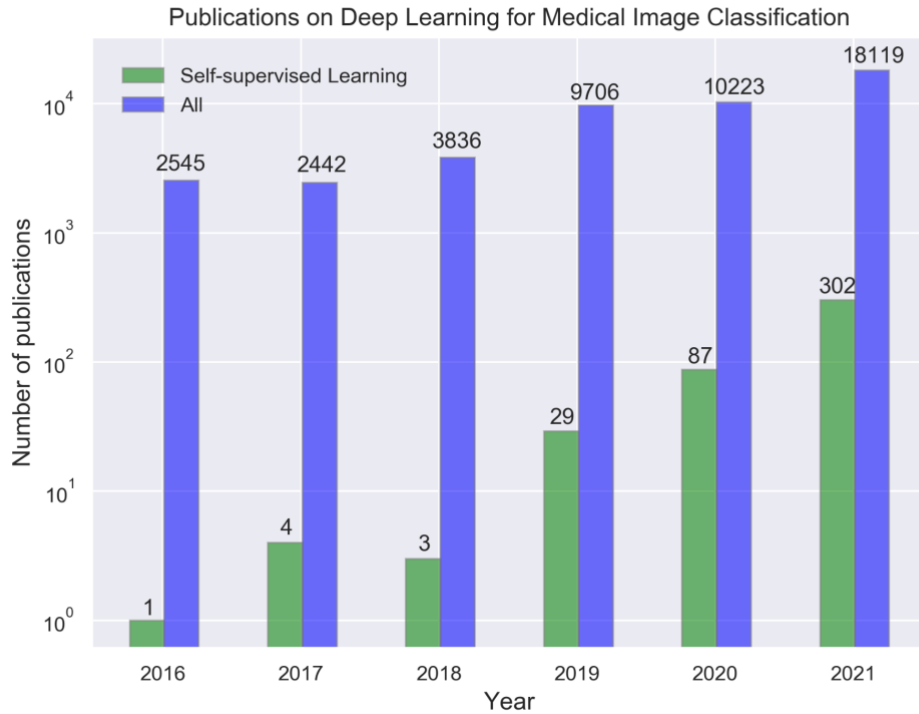


*Figure 1. Timeline showing number of publications on deep learning for medical image classification per year, found by using the same search criteria on PubMed, Scopus and ArXiv. The figure shows that self-supervised learning is a rapidly growing subset of deep learning for medical imaging literature.*

## Terminology and strategies in self-supervised learning

Here we provide definitions for different categorizations of self-supervision strategies, namely innate relationship, generative, contrastive, and self-prediction (Figure 2)<sup>23</sup>. The relative ordering of these self-supervision strategies is based on the chronological order in which they were popularized. It is worth noting that some definitions can be overlapping since clear distinctions between each method can not always be made.

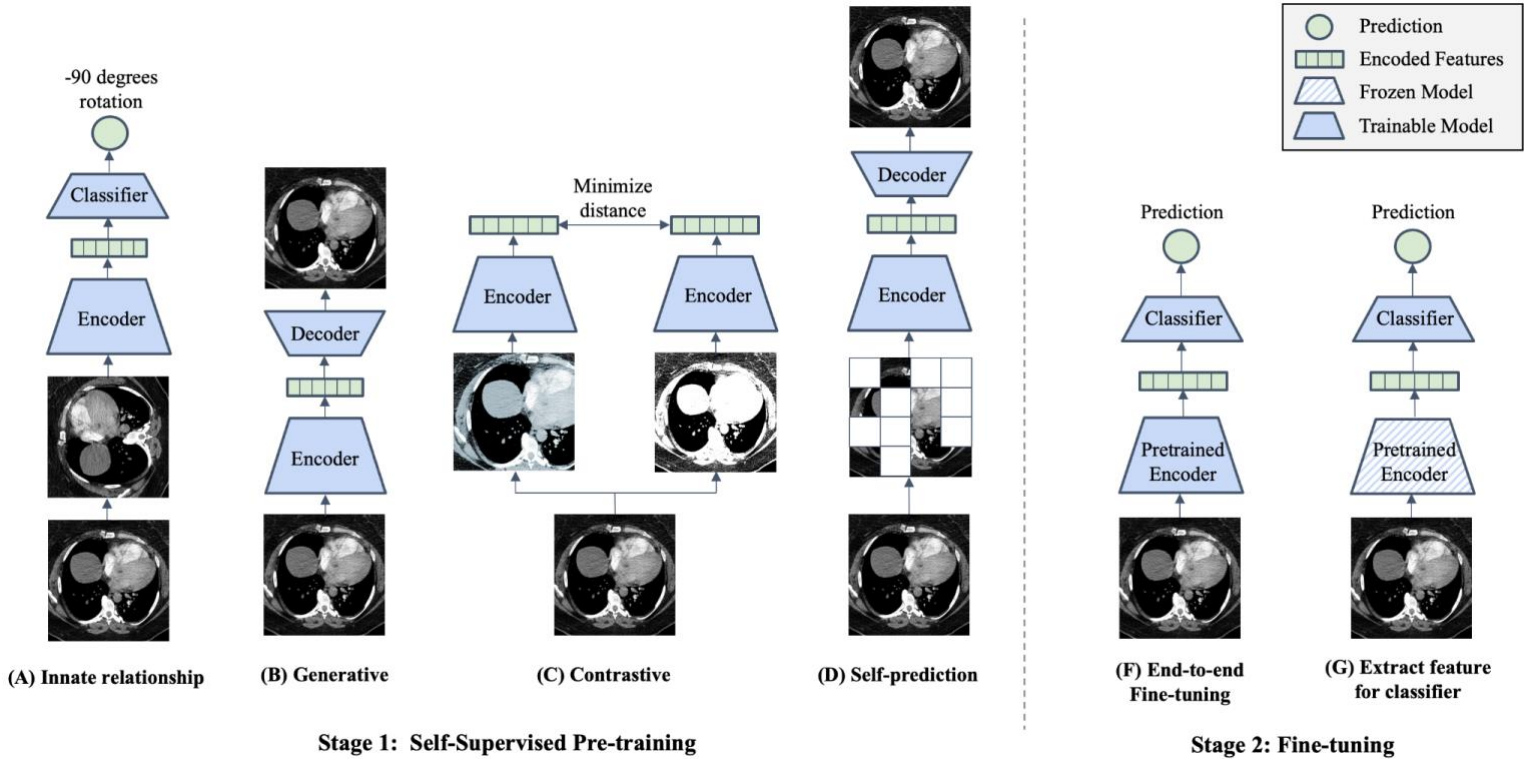


Figure 2: Illustration of different self-supervised learning and fine-tuning strategies. During **Stage 1** a model is pre-trained using one or more of the following self-supervised learning strategies: (a) Innate relationship SSL pretrains a model on a hand-crafted task by leveraging the internal structure of the data, (b) Generative SSL learns the distribution of training data, enabling reconstruction of the original input (c) Contrastive SSL forms positive pairs between different augmentations of the same image and minimizes representational distances of positive samples closer together (d) Self-prediction augments or masks out random portions of an image, and reconstructs the original image based on the unaltered parts of the original image. During **Stage 2**, the pre-trained model can be fine-tuned using one of the following strategies: (f) end-to-end fine-tuning of the pre-trained model and classifier, or (g) train a classifier which uses extracted features from the SSL pre-trained model.

### Innate relationship

Innate relationship SSL is the process of pretraining a model on a hand-crafted task which can leverage the internal structure of the data, without acquiring additional labels. In the most general sense, innate relationship models perform classification or regression based on the hand-crafted task instead of optimizing based on the model's ability to reconstruct (Generative and Self-prediction) or represent the original image (Contrastive). Specifically, these methods are optimized using classification or regression loss derived from the given task. Pretraining the model on such a hand-crafted task makes the model learn visual features as a starting point. However, innate relationship SSL can lead to visual features that are effective only for the hand-crafted task but have limited benefits for the downstream task. Examples of innate relationship for visual inputs include predicting image rotation angle<sup>24</sup>, solving jigsaw puzzles of an image<sup>25</sup>, or determining the relative positions of image patches<sup>26</sup>.

## Generative

Generative models, popularized through the advent of traditional autoencoders<sup>27</sup>, variational autoencoders<sup>28</sup> and generative adversarial networks (GANs)<sup>29</sup>, are able to learn the distribution of training data, and thereby reconstruct the original input or create new synthetic data instances. By using readily available data as the target, generative models can be trained to automatically learn useful latent representations without the need for explicit labels, and thus constitute a form of self-supervision. Early work that leverages generative models for self-supervised learning rely on autoencoders, where an encoder converts inputs into latent representations and a decoder reconstructs the representation back to the original image<sup>30</sup>. Subsequently, these models are optimized based on how closely the reconstructed images resemble the original image. More recent work has explored utilizing GANs for generative self-supervised learning, with improvement in performance over prior work<sup>31,32</sup>.

## Contrastive

Contrastive self-supervised methods are based on the assumption that variations caused by transforming an image do not alter the image's semantic meaning. Therefore different augmentations of the same image constitute a so-called positive pair, while the other images and their augmentations are defined to be negative pairs in relation to the current instance. Subsequently a model is optimized to minimize the latent space distances between the positive pairs and push apart negative samples. Separating representations for positive and negative pairs can be based on arbitrary distance metrics incorporated into the contrastive loss function. One pioneering contrastive-based method is SimCLR<sup>20</sup>, which outperformed supervised models on ImageNet benchmark using 100 times fewer labels. However, SimCLR requires a very large batch size to perform well, which can be computationally prohibitive for most researchers. To reduce the large batch size required by SimCLR to ensure enough informative negative samples, Momentum Contrast (MoCo) introduced a momentum encoded queue to keep negative samples<sup>33</sup>. More recently, a subtype of contrastive self-supervised learning called instance discrimination, which includes methods such as DINO<sup>34</sup>, BYOL<sup>35</sup> and SimSiam<sup>36</sup>, further eliminates the need for negative samples. Instead of contrastive augmented pairs from the same image, several studies have explored contrasting clustering assignments of augmented versions of the same image<sup>37-39</sup>.

## Self-prediction

Self-prediction SSL is the process of masking or augmenting portions of the input and using the unaltered portions to reconstruct the original input. The idea of self-prediction self-supervised learning originated from the field of Natural Language Processing (NLP), where state-of-the-art models were pre-trained using the Masked Language Modeling approach by predicting missing words in a sentence<sup>18,19</sup>. Motivated by the success in NLP, early work in the field of computer vision made similar attempts by masking out or augmenting random patches of an image and training Convolutional Neural Networks (CNNs) to reconstruct the missing regions as a pre-training strategy<sup>40</sup> but only with moderate success. Recently, the introduction of Vision Transformers (ViT) allowed computer vision models to also have the same transformer-based architecture. Studies such as BERT Pre-Training of Image Transformers (BEiT) and Masked Auto-encoders (MAE), which combine ViT with self-prediction pre-training objective, achieve state-of-the-art results when fine-tuned across several natural image benchmarks<sup>41,42</sup>. Similar to generative SSL, self-prediction models are optimized using the reconstruction loss. The key difference between self-prediction and generative self-supervised learning methods is that self-prediction applies masking or

augmentations only to portions of the input image, and uses the remaining, unaltered portions to inform reconstruction. On the other hand, generative based self-supervised learning either applies augmentations on the whole image or does not apply any augmentations.

### Strategies for fine-tuning

There are two main strategies for fine-tuning models that have been pre-trained using SSL (Figure 2). If we consider any imaging model to be composed of an encoder part and a classifier part, then these two strategies are 1) end-to-end fine-tuning vs. 2) extract features from the encoder first and subsequently train an additional classifier. In end-to-end fine-tuning all the weights of the encoder and classifier are unfrozen and can be adjusted through optimization using supervised learning in the fine-tuning phase. In the feature-extraction strategy, the weights of the encoder are kept frozen to extract features as inputs to the downstream classifier. While many previous work uses linear classifiers with trainable weights (also known as linear probing), any type of classifier or architecture can be used, including SVMs or even non-trainable classifiers such as k-nearest neighbor<sup>43</sup>. It is worth emphasizing that SSL is task agnostic, and the same SSL pretrained model can be fine-tuned for different types of downstream tasks, including classification, segmentation, and object detection.

### Results

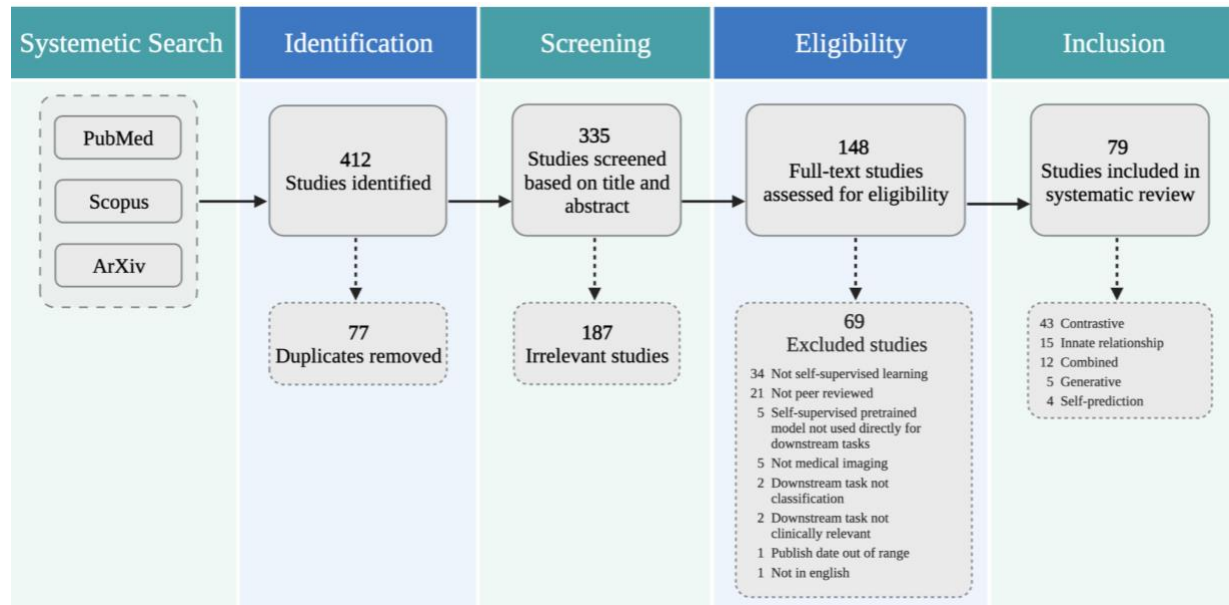
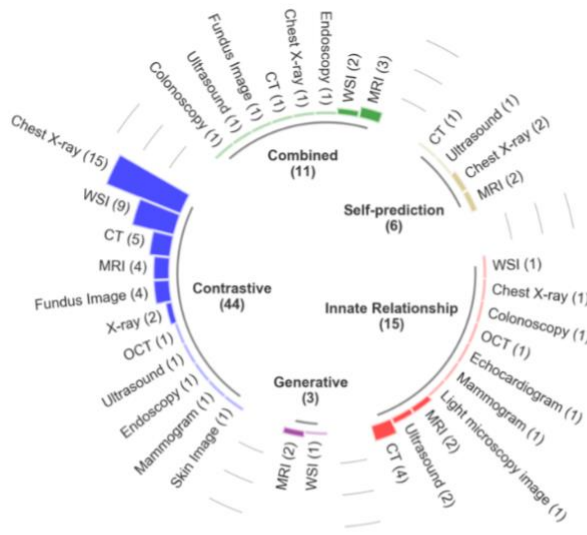
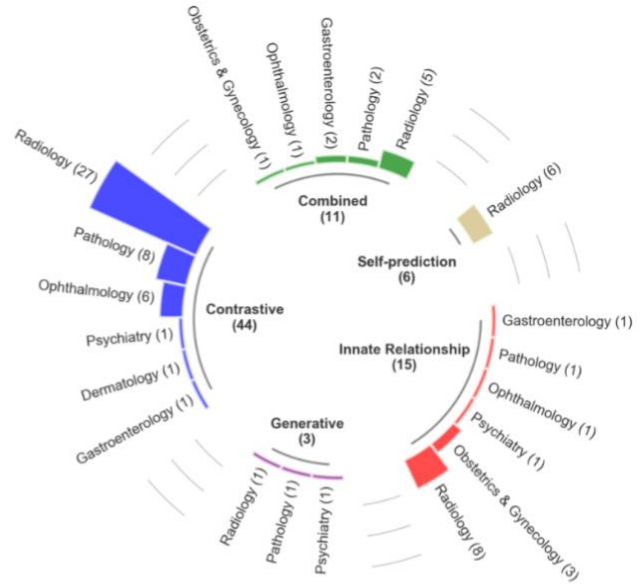


Figure 2. Authors independently screened all records for eligibility. Out of 412 studies identified from PubMed, Scopus, and ArXiv, 79 studies were included in the systematic review.

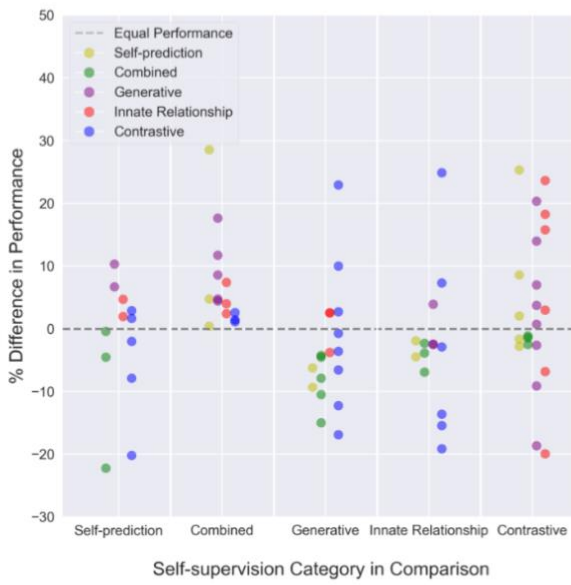
A total of 412 unique studies were identified through our systematic search. After removing duplicates and excluding studies based on title and abstract using our study selection criteria (see Methods), 148 studies remained for full-text screening. A total of 79 studies fulfilled our eligibility criteria and were included for systematic review and data extraction. Figure 2 presents a flowchart of the study screening and selection process. Table 1 displays the included studies and extracted data while Figure 3 summarizes the statistics of extracted data.



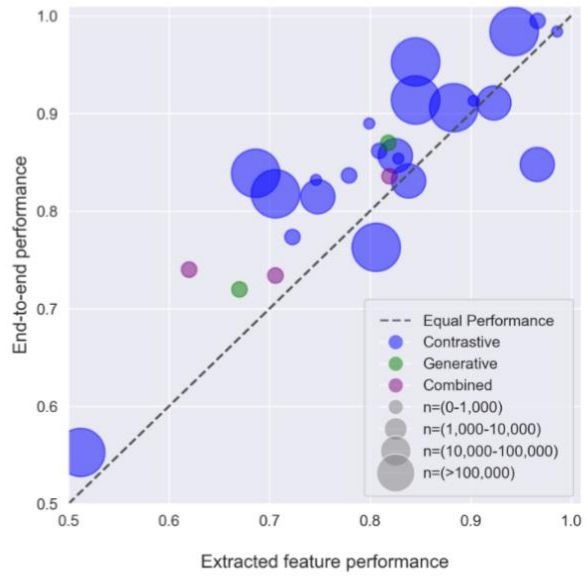
(A)



(B)



(C)



(D)



*Figure 3. Summary of extracted data from studies in our system review. A) Prevalence of different medical specialties split by self-supervised learning strategy. B) Prevalence of different medical imaging modalities split by self-supervised learning strategy. C) Relative performance difference between different types of self-supervised learning strategies on the same task. D) Performance comparison between end-to-end fine-tuning vs. training a classifier using extracted features from pretrained self-supervised models. E) Relative difference in downstream task performance between self-supervised and non-self-supervised models.*



## 1 Innate Relationship

2 Innate relationship was used in 15 out of 79 studies (Table 1). Nine of these studies designed their innate  
3 relationship pre-text task based on different image transformations, including rotation prediction<sup>107–110</sup>,  
4 horizontal flip prediction<sup>103</sup>, reordering shuffled slices<sup>105</sup>, and patch order prediction<sup>104,109,112,113</sup>. Notably,  
5 Jiao et al. pre-trained their models simultaneously with two innate relationship pre-text tasks (slice order  
6 prediction and geometric transformation prediction), and showed that a weight-sharing Siamese network  
7 out-performs a single disentangled model for combining the two pre-training objectives<sup>46</sup>. The remaining  
8 six studies designed clinically relevant pretext tasks by exploiting the unique properties of medical images.  
9 For instance, Droste et al. utilized a gaze tracking dataset and pre-trained a model to predict sonographers’  
10 gazes on ultrasound video frames with gaze-point regression<sup>102</sup>. Dezaki et al. employed temporal and spatial  
11 consistency to produce features for echocardiograms that are strongly correlated with the heart’s inherent  
12 cyclic pattern<sup>111</sup>. Out of all innate relationship based studies, ten compared performance to those of  
13 supervised pre-trained models and eight of them showed improvement in performance. On average,  
14 clinically relevant pre-text tasks achieved greater improvements in performance over transformation-based  
15 pre-text tasks, when compared to purely supervised methods (13.7% vs 5.03%).

## 16 Generative

17 Generative self-supervised learning was used in 3 out of 79 studies (Table 1). Gamper et al. extracted  
18 histopathology images from textbooks and published papers along with the figure captions and devised an  
19 image captioning task for self-supervised pre-training, where a ResNet-18 was used for encoding images,  
20 and the representation was fed to transformers for image-captioning<sup>100</sup>. They were subsequently able to use  
21 the learned representations for a number of downstream histopathology tasks, including breast cancer  
22 classification. Osin et al.<sup>98</sup> leveraged the chronology of sequential images in brain fMRI for self-supervised  
23 pre-training. Brain fMRI scans are typically acquired with subjects alternating between a passive and an  
24 active phase, where the subject is instructed to perform some task or receives some external stimulus.  
25 During the self-supervision phase, Osin et al. trained two networks: an autoencoder to generate the active  
26 fMRI image given the passive image, and an LSTM to predict the next active image. The representations  
27 learned during the self-supervision were then used to train a classifier to predict psychiatric traits such as  
28 post-traumatic stress disorder (PTSD). Finally, Zhao et al. use a generative approach with an autoencoder  
29 with an additional constraint that explicitly associates brain age to the latent representations for  
30 longitudinally acquired brain MRIs<sup>99</sup>. Of the three studies, two reported comparisons with purely supervised  
31 models and showed relative improvements of 16.6%<sup>99</sup> and 24.5%<sup>100</sup> with self-supervised learning.

## 33 Contrastive

34 The majority of the studies that remained after our full-text screening (44/79) used contrastive learning as  
35 their self-supervised pre-training strategy (Table 1). SimCLR, MoCo and BYOL were the three most used  
36 frameworks, applied in 13, 8 and 3 papers respectively. Some papers leveraged medical domain priors to  
37 create specialized strategies for creating positive pairs. For pathology slices, Li et al. exploited that the  
38 neighborhood around a patch is likely to be similar, and used pre-clustering to find dissimilar patches<sup>62</sup>. In  
39 radiology, Ji et al. used multimodal contrastive learning by matching X-rays with corresponding radiology  
40 reports<sup>76</sup>. They extracted and fused the representations of the image and text modalities through both global  
41 image-sentence matching and local attention-based region-phrase matching. Wang et al. utilized both

42 radiomic features and deep features from the same image to form positive pairs<sup>93</sup>. They also utilized the  
43 spatial information of the patches, by mining positive pairs from proximate tumor areas and negative pairs  
44 from distant tumor areas. Dufumier et al. (2021) used patient meta-data from MRI to form positive pairs<sup>84</sup>.  
45 36 studies compared contrastive SSL pre-training to supervised pre-training, and reported an average  
46 improvement in performance of 6.35%.

#### 47 Self-prediction

48 Self-prediction was used in six out of all included studies (Table 1). We consider studies that applied local-  
49 pixel shuffling as self-prediction since the augmentation operation, which shuffles the order of pixels, is  
50 applied only to a random patch of an image. Liu et al. used a U-net model to restore Ultrasound images  
51 augmented with local-pixel shuffling, and they subsequently concatenated the outputs of the U-net encoder  
52 with featurized clinical variables (age, gender, tumor size) for the downstream prediction task<sup>121</sup>. Similarly,  
53 Zhong et al. designed three image restoration tasks on cine-MRI videos and used a U-net-like encoder-  
54 decoder architecture including skip connections to perform the image restoration<sup>119</sup>. Three different image  
55 restoration tasks were set up using local-pixel shuffling, within-frame pixel shuffling, and covering an entire  
56 video frame with random pixels. Jana et al. used an encoder-decoder architecture for image restoration of  
57 CT scans that were corrupted by swapping several small patches within a single CT slice<sup>118</sup>. Jung et al.  
58 created a functional connectivity matrix between pairs of region-of-interest in rs-fMRI for each subject, and  
59 created a masked auto-encoder task by randomly masking out different rows and columns of the matrix for  
60 restoration<sup>120</sup>. Two of the five studies compared their approach to models without self-supervised pre-  
61 training and reported slight relative improvements in performance of 1.12%<sup>117</sup> and 0.690%<sup>121</sup>.

#### 62 Combined Approaches

63 Eleven studies found creative ways to combine different self-supervised learning strategies to pretrain their  
64 medical imaging models (Table 1). Over half of these studies (6/11) combined contrastive with generative  
65 approaches. With the exception of Ke et al.'s work<sup>53</sup>, which uses a CycleGAN for histopathology slide stain  
66 normalization, all studies utilized an autoencoder as their generative model when combined with contrastive  
67 strategies. A combination of contrastive and innate relationships was used in three studies. The innate  
68 relationship tasks range from augmentation prediction and patch positioning prediction<sup>122</sup>, rotation  
69 prediction<sup>50</sup>, and ultrasound video to speech correspondence prediction<sup>46</sup>. For the remaining two studies,  
70 Cornelissen et al. used a conditional GAN, and trained the generator network on endoscopic images of the  
71 esophagus to either recolorize, inpaint and generate super-resolution images<sup>49</sup>. Because their tasks consisted  
72 of both inpainting (self-prediction) and super-resolution (generative), their approach was considered  
73 combined. Haghghi et al. combined three different SSL strategies (generative, innate relationship, self-  
74 prediction) by first training an auto-encoder and group instances with similar appearances based on the  
75 latent representations from the auto-encoder<sup>48</sup>. Then, the authors randomly cropped image patches at a fixed  
76 coordinate for all instances in the same group, and assigned a pseudo label to the cropped patches at each  
77 coordinate. Finally, the cropped patches were randomly perturbed and a restoration autoencoder was trained  
78 simultaneously with a pseudo label classification objective. Eight of the studies that combined different  
79 strategies compared self-supervised pre-training with purely supervised approaches, all of which reported  
80 performance improvement (0.140%-8.29%).

## 81 Discussion

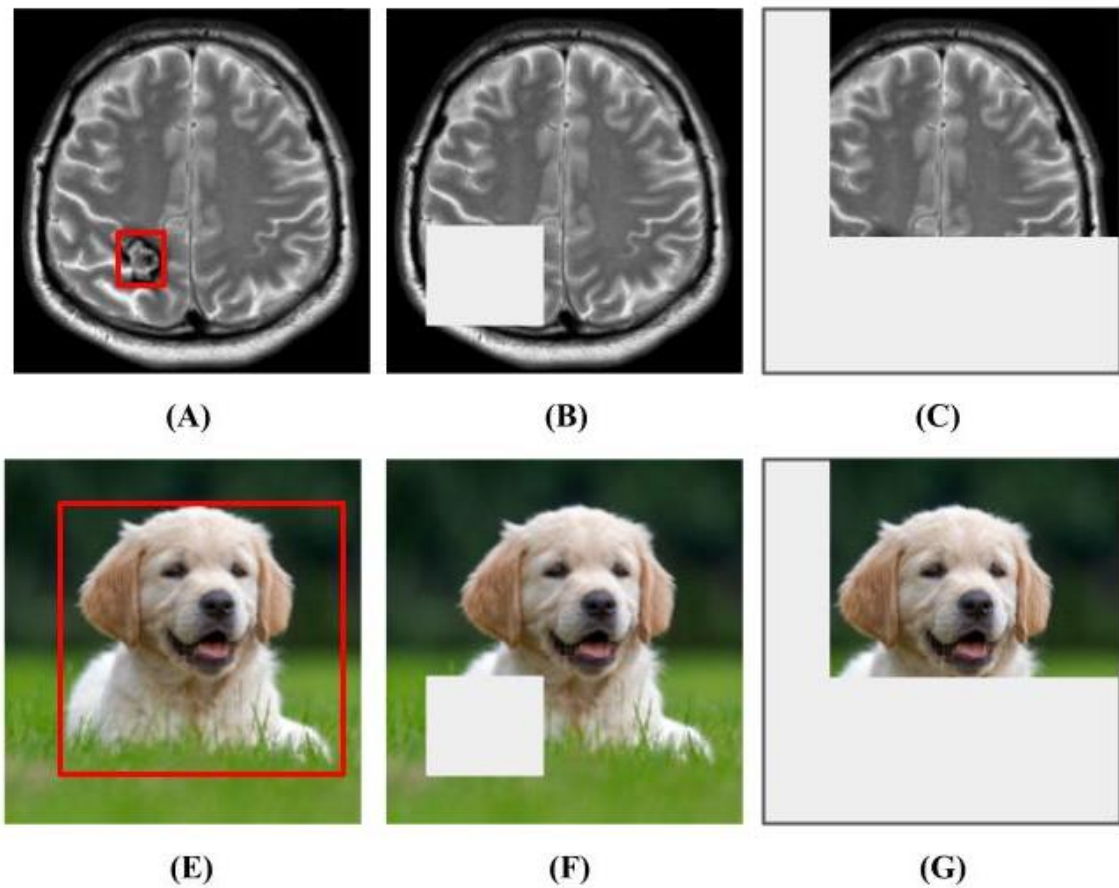
82 This review aims to aggregate the collective knowledge of prior works that applied SSL to medical  
83 classification tasks. By synthesizing the relevant literature, we provide consistent definitions for self-  
84 supervised learning techniques, categorize prior works by their pre-training strategies, and provide  
85 implementation guidelines based on lessons learned from prior works. While five studies reported a slight  
86 decrease in performance (0.980%-4.51%), the majority of self-supervised pretrained models led to relative  
87 increased performances of 0.216–32.6% AUROC, 0.440–29.2% accuracy, and 0.137-14.3% F1 score over  
88 the same model architecture without SSL pretraining, including both ImageNet and random initialization  
89 (Figure 3E). In Figure 3C we show a comparison of different SSL strategies on the same downstream task,  
90 which suggests that a combined strategy tends to outperform other self-supervised categories. However, it  
91 is important to note that combined strategies are typically the proposed method in the manuscripts, and thus  
92 publication bias might have resulted in this trend. In Figure 3D we additionally plot the performance of the  
93 two main types of fine-tuning strategies on the same task, and the graph tends to indicate that end-to-end  
94 fine-tuning leads to better performance regardless of the dataset size. In the presence of relevant data, we  
95 recommend implementing self-supervised learning strategies for training medical image classification  
96 models since our literature review indicated that self-supervised pre-training generally results in better  
97 model performance, especially when annotations are limited (Table 1).

98  
99 The types of medical images utilized for model development as well as the downstream classification task  
100 encompassed a wide range of medical domains and applications (Figure 3A&B). The vast majority of the  
101 studies explored the clinical domain of radiology (47/79), of which 27 were focused on investigating  
102 abnormalities on chest imaging such as pneumonia, COVID-19, pleural effusion and pulmonary embolism  
103 (see Table 1). The choice of this domain is likely a combination of the availability of large-scale public  
104 chest datasets such as CheXpert<sup>123</sup>, RSPECT<sup>124</sup>, RadFusion<sup>125</sup> and MIMIC-CXR<sup>126</sup>, as well as the  
105 motivation to solve acute or emerging healthcare threats which was the case during the coronavirus  
106 pandemic<sup>57,67,68,70,97,103,106,108,109,117,127</sup>. The second most prevalent clinical domain was pathology (12/79).  
107 Similar to radiology, this field is centered around medical imaging in the form of whole slide images. The  
108 tasks were focused on histopathological classification, where the majority focused on colorectal cancer  
109 classification<sup>53,54,64,91,115</sup>. The remaining studies explored multiple other tasks and many focused on  
110 classification of malignant disorders such as breast cancer<sup>63,93,100</sup>, skin cancer<sup>128</sup>, and lung cancer<sup>62</sup>. A  
111 particularly interesting medical task that was explored was classification of psychiatric diseases or  
112 psychiatric traits using fMRI<sup>84,98,114</sup>. Current limited knowledge and understanding of possible imaging  
113 features arising in psychiatric diseases constitutes a major clinical challenge to making local annotations  
114 such as bounding boxes or segmentations on brain scans. In this case both Osin et al. and Hashimoto  
115 demonstrated that training a self-supervised framework could be beneficial to generate representative latent  
116 features of brain fMRIs before fine-tuning on image-level class labels<sup>98,114</sup>.

117  
118 A majority of the included studies lacked strong baselines and ablation experiments. Even though 60 out of  
119 79 studies compared their results with purely supervised baselines, only 33 studies reported comparisons  
120 with another self-supervised learning strategy. Of the 33 studies, 26 compared with a self-supervised  
121 category that differs from their best performing model. Among the SSL baselines, SimCLR was most  
122 frequently compared (16/26), followed by autoencoders (11/26) and MoCo (9/26). Furthermore, only 18  
123 out of 79 studies indicated use of natural image pre-trained weights, either supervised or self-supervised, to

124 initiate their model for subsequent in-domain self-supervised pre-training. Lastly, merely 13 studies  
125 compared performance between classification on extracted features to end-to-end fine-tuning, two of which  
126 did not report numerical results. Of the 11 studies that quantitatively reported performance, eight found  
127 end-to-end fine-tuning to outperform training a new classifier on extracting features (Figure 3d). Since self-  
128 supervised learning for medical images is a promising yet nascent research area and the optimal strategies  
129 for training these models are still to be explored, researchers should systematically investigate different  
130 categories of self-supervised learning for their medical image datasets, in addition to fine-tuning strategy  
131 and pre-trained weights. Researchers should also test their newly developed strategies on multiple datasets,  
132 ideally on different modalities and medical imaging domains.

133



134  
135 *Figure 4. Examples of augmentations and transformations that alter the semantic meaning of medical*  
136 *images<sup>129</sup> but not natural images<sup>130</sup>. A) The image shows a T2-weighted brain MRI with a cavernoma in*  
137 *the right parietal lobe (bounded in red). B) and C) Masking and cropping operations can obscure the*  
138 *cavernoma and alter the semantic meaning of the image, as the MRI-scan no longer exhibits any*  
139 *abnormality. E) Image of a dog (bounded in red), F) and G) Masking and cropping operations do not*  
140 *obscure the dog nor alter the semantic meaning of the image.*

141

## 142 Implementation guidelines for self-supervised learning models

143 Definitive conclusions on the optimal strategy for medical images cannot be made since only a subset of  
144 studies made comparisons between different types of self-supervised learning strategies. Furthermore, the  
145 optimal strategy may be dependent on a number of factors including the specific medical imaging domain,  
146 the size and complexity of the dataset, and the type of classification task<sup>131,132</sup>. Due to this heterogeneity,  
147 we encourage researchers to compare multiple self-supervised learning strategies for developing medical  
148 image classification models, especially in limited data regimes. Although self-supervised pre-training can  
149 be computational demanding, many models pre-trained in a self-supervised manner on large-scale natural  
150 image datasets are publicly available and should be utilized. Azizi et al. have shown that models that are  
151 SSL pre-trained using natural images tend to outperform purely supervised pre-trained models<sup>72</sup> for medical  
152 image classification, and continuing self-supervised pre-training with in-domain medical images leads to  
153 the best results. More recently, Azizi et al. found that using generic and large-scale *supervised* pretrained  
154 models, such as BigTransfer<sup>133</sup>, can also benefit subsequent domain-specific self-supervised pre-training,  
155 and ultimately improve model performance and robustness for different medical imaging modalities<sup>134</sup>.  
156 Truong et al. have demonstrated the effectiveness of combining representations from multiple self-  
157 supervised methods to improve performance for three different medical imaging modalities<sup>73</sup>.

158  
159 It is worth noting that representations learned using certain SSL strategies can be relatively more linearly  
160 separable, while representations from other strategies can achieve better performance when more layers or  
161 the entire model are fine-tuned. For instance, for natural image datasets, MoCo outperforms MAE by  
162 training a linear model on extracted features (linear probing), while MAE achieves better performance than  
163 MoCo as the number of fine-tune layers increases<sup>41</sup>. Likewise, Cornelissen et al. demonstrated that using  
164 representations from earlier layers can improve downstream classification of neoplasia in Barrett’s  
165 Esophagus<sup>49</sup>. Factors such as the degree of domain shift between SSL pre-training data and downstream  
166 task data could also affect the linear separability of the representations. Based on our aggregated results,  
167 we found that end-to-end fine-tuning generally leads to better performance for medical images (Figure 3C).  
168 However, due to the lack of ablation studies from current work, we cannot determine whether fine-tuning  
169 only later layers of the model could lead to better performance, relative to end-to-end fine-tuning.  
170 Furthermore, even though self-supervised learning strategies generate label-efficient representations, the  
171 learning process typically requires a relatively large amount of unlabeled data. For instance, reducing the  
172 number of pre-training images from 250k to 50k typically leads to more than 10.0% drop in accuracy for  
173 downstream tasks, while reducing from 1M to 250k leads to a 2.00-4.00% decrease<sup>132</sup>. Curating large-scale  
174 medical image datasets from multiple institutions is often challenged by the difficulty of sharing patient  
175 data while preserving patient privacy. Nevertheless, Yan et al. have demonstrated the possibility of training  
176 self-supervised models with data from multiple healthcare centers without the need for explicitly sharing  
177 data using federated learning, and shown improvement in robustness and performance over models trained  
178 using data from only one institution<sup>135</sup>.

179  
180 The field of self-supervised learning for computer vision is constantly and rapidly evolving. While many  
181 self-supervised methods have led to state-of-the-art results when fine-tuned on natural image datasets, how  
182 translatable these results are to medical datasets is unclear, mainly due to the unique properties of medical  
183 images. For instance, many contrastive based strategies have been developed based on the assumption that  
184 the class-defining object is the main focus of an image, and thus variations caused by image transformations  
185 should not alter the image’s semantic meanings (Figure 4). Therefore, these methods typically apply strong

186 transformations to the original image and encourage the model to learn similar global representations for  
187 images with similar semantic meanings. However, the assumption made for natural images is not  
188 necessarily valid for medical images for two reasons. First, medical images have high inter-class visual  
189 similarities due to the standardized protocols for medical image acquisition and the homogeneous nature of  
190 human anatomy. Second, within the medical imaging domain, the semantic meaning of interest is rarely an  
191 object such as the anatomical organ, but is rather the presence or absence of pathological abnormalities  
192 within that organ or tissue. Many abnormalities are characterized by very subtle and localized visual cues,  
193 which can become ambiguous or obscured by augmentations (Figure 4c). The random masking operation  
194 often utilized by self-prediction self-supervised learning methods may also alter a medical image's semantic  
195 meaning by removing image regions with diseases or abnormalities (Figure 4b). Recent work has  
196 demonstrated the benefit of using learned visual word masks<sup>136,137</sup> or spatially constrained crops<sup>138,139</sup> to  
197 encourage representational invariance with semantically more similar regions of an image. In a similar vein,  
198 we believe that augmentation strategies tailored for the nature of medical images during self-supervised  
199 learning is a future research area that warrants further research and exploration.

200  
201 The unique properties of medical images can be leveraged to design self-supervised learning methods more  
202 suitable for specific downstream tasks. For instance, instead of forming positive pairs with different  
203 augmented versions of the same image during contrastive learning, one can improve positive sampling  
204 according to the similarity between a patient's clinical information. In fact, several studies have shown  
205 performance improvement when constructing positive pairs with slices from the same CT series<sup>77</sup>, images  
206 from the same imaging study<sup>75</sup>, images from the same patient<sup>72</sup> and patients with similar age<sup>84</sup>. Future  
207 research should explore other strategies for defining positive pairs, such as leveraging patient demographics  
208 or medical history information. The unique attributes of medical images can also be utilized for creating  
209 relevant pretext tasks. Rivail et al. proposed a self-supervised approach to model disease progression by  
210 estimating the time interval between pairs of optical coherence tomography (OCT) scans from the same  
211 patient<sup>101</sup>. Involving additional modalities during self-supervised learning has also been shown to improve  
212 a model's performance when fine-tuned for downstream tasks. For example, Taleb et al. proposed a  
213 multimodal contrastive learning strategy between retinal fundus images and genetics data and showed  
214 improvement in performance over single modality pre-training<sup>140</sup>. Jiao et al. cleverly leveraged the  
215 correlation between fetal ultrasonography and the narrative speech of the sonographer to create a pretext  
216 task for self-supervision, and subsequently used the learned representations for downstream standard plane  
217 classification on sonograms<sup>46</sup>. Furthermore, many medical imaging modalities have corresponding  
218 radiology reports that contain detailed descriptions of the medical conditions observed by radiologists.  
219 Several studies have utilized these medical reports to provide supervision signals during self-supervised  
220 learning and shown label efficiency for downstream tasks<sup>76,141</sup>. By leveraging radiology reports, Huang et  
221 al. demonstrated the model's ability to localize chest abnormalities on chest x-rays without segmentation  
222 labels and revealed the possibility of zero-shot learning by converting the classification classes into textual  
223 captions and framing the image classification task as measuring the image-text similarity<sup>142</sup>. However,  
224 currently there are very few publicly available medical image datasets with corresponding radiology  
225 reports, largely due to the difficulties in preserving patient privacy. Therefore, these multi-modal self-  
226 supervised learning strategies are limited to implementation within a healthcare system until more datasets  
227 with medical image and report pairs are publicly released. Overall, the flexibility in creating self-supervised  
228 methods as well as the adaptability and transferability to multiple medical domains highlights the  
229 importance and utility of self-supervised techniques in clinical applications.

## 230 Limitations

231 For this review paper, publication bias can be a considerable limitation due to disproportionately reported  
232 positive results in the literature, which can lead to overestimation of the benefits of self-supervised learning.  
233 We also limited our search to only consider papers published after 2012, which excluded papers that applied  
234 self-supervised learning prior to the era of deep learning for computer vision<sup>143</sup>. Furthermore, we are unable  
235 to aggregate or statistically compare the effects of each self-supervised learning strategy on performance  
236 gain, since the included studies use different imaging modalities, report different performance metrics, and  
237 investigate different objectives. Additionally, subjectivity may have been introduced when categorizing the  
238 self-supervised learning strategy in each paper, especially for studies that implemented novel,  
239 unconventional, or a mixture of methods. Lastly, our study selection criteria only included literature for the  
240 task of medical image classification, which limits the scope of this review paper, since we recognize that  
241 self-supervised pretrained models can also be finetuned for other important medical tasks, including  
242 segmentation, regression, and registration.

## 243 Future Research

244 Results from this systematic review have revealed that SSL for medical image classification is a growing  
245 and promising field of research across multiple medical disciplines and imaging modalities. We found that  
246 self-supervised pre-training generally improves performance for medical imaging classification tasks over  
247 purely supervised methods. We categorized the SSL approaches used in medical imaging tasks as a  
248 framework for methodologic communication and synthesized benefits and limitations from literature to  
249 provide recommendations for future research. Future studies should include direct comparisons of different  
250 self-supervised learning strategies using shared terminology and metrics whenever applicable to facilitate  
251 the discovery of additional insights and optimal approaches.

## 252 Methods

253 This systematic review was conducted based on the PRISMA guidelines<sup>144</sup>.

## 254 Search Strategy

255 A systematic literature search was implemented in three literature databases: PubMed, Scopus and ArXiv.  
256 The key search terms were based on a combination of two major themes: “self-supervised learning” and  
257 “medical imaging”. Search terms for medical imaging were not limited to radiological imaging but were  
258 also broadly defined to include imaging from all medical fields, i.e., fundus photography, whole slide  
259 imaging, endoscopy, echocardiography, etc. Since we specifically wanted to review literature on the task  
260 of medical image classification, terms for other computer vision tasks such as segmentation, image  
261 reconstruction, denoising and object detection were used as exclusion criteria in the search. The search  
262 encompassed papers published between January, 2012 and May 2021. The start date was considered  
263 appropriate due to the rising popularity of deep learning for computer vision since the 2012 ImageNet  
264 challenge. The complete search string for all three databases is provided in Supplementary Methods.

265  
266 We included all research papers in English that used self-supervision techniques to develop deep learning  
267 models for medical image classification tasks. The research papers had to be original research in the form  
268 of either journal articles, conference proceedings or extended abstracts. We excluded any publications that

269 were not peer-reviewed. Applicable self-supervision techniques were defined according to the different  
270 types presented in the “terminology and strategies in self-supervised learning” section. We only included  
271 studies that applied the deep learning models to a downstream medical image classification task, i.e, it was  
272 not sufficient to have developed a self-supervision model on medical images. Additionally, the medical  
273 image classification task had to be a clinical task or clinically relevant task. For example, the downstream  
274 task of classifying the frame number in a temporal sequence of frames from echocardiography<sup>145</sup> was not  
275 considered a clinically relevant task.

276  
277 We excluded studies that used semi-supervised learning or any amount of manually curated labels during  
278 the self-supervision step. We also excluded studies that only investigated regression or segmentation in  
279 their downstream tasks. Furthermore, we excluded any studies where the self-supervised pretrained model  
280 was not directly fine-tuned for classification after pretraining. Studies that used non-human medical  
281 imaging data (i.e., veterinarian medical images) were also excluded.

282

## 283 **Study Selection**

284 The Covidence software ([www.covidence.org](http://www.covidence.org)) was used for screening and study selection. After the  
285 removal of duplicates, studies were screened based on title and abstract, and then full texts were obtained  
286 and assessed for inclusion. Study selection was performed by three independent researchers (S.-C.H., A.P.,  
287 and M.J.), and disagreements were resolved through discussion. In cases where consensus could not be  
288 achieved a forth arbitrating researcher was consulted (A.S.C.).

289

## 290 **Data Extraction**

291 For benchmarking the existing approaches we extracted the following data from each of the selected  
292 articles: a) self-supervised learning strategy, b) year of publication, c) first author, d) imaging modality, e)  
293 clinical domain, f) outcome/task, g) combined method, h) self-supervised framework, i) strategy for fine-  
294 tuning, j) performance metrics, k) SSL performance, l) supervised performance, and m) difference in SSL  
295 and supervised performance (Table 1). We also computed the relative difference in performance between  
296 the supervised and self-supervised model on the p) full dataset and q) subset. We classified the specific  
297 self-supervised learning strategy based on the definitions in the section “Terminology and strategies in self-  
298 supervised learning”. We extracted AUROC whenever this metric was reported, otherwise we prioritize  
299 accuracy over F1 score and sensitivity. When the article contained results from multiple models (i.e. ResNet  
300 and DenseNet), metrics from the experiment with the best average performing self-supervised model were  
301 extracted. When the authors present results from several clinical tasks, we chose tasks that best  
302 corresponded to the title and objective of the manuscript. If the tasks were deemed equal, we picked the  
303 task where the chosen SSL model had the highest performance. We picked supervised baseline with the  
304 same model architecture and pre-training dataset for performance comparison. If the author did not report  
305 performance from a supervised model that uses the same pre-training dataset, preference was given to  
306 ImageNet pretrained model over a randomly initialized one. The pre-training dataset used by the self-  
307 supervised and supervised model are recorded in the Supplementary Table. When papers report results on  
308 many percentages of fine-tuning (i.e., 1%, 10%, 100%), we pick the lowest and highest to study the label-  
309 efficiency of self-supervised learning methods. We also provide a Supplementary Table 1 with additional



310 technical details including model architecture, dataset details, number of training samples, comparison to  
311 selected baselines and performance on subsets of data. These items were extracted to enable researchers to  
312 find and compare current self-supervised studies in their medical field or input modalities of interest.

### 313 Data Availability

314 The authors declare that all data supporting the findings of this study are available within the paper and its  
315 Supplementary information files.

### 316 Contributions

317 S.-C.H. and A.P. are co-first authors who contributed equally to this study. Concept and design: S.-C.H.  
318 and A.P.. Study selection: S.-C.H. and A.P. Data extraction: S.-C.H., A.P., and M.J. Drafting of the  
319 manuscript: S.-C.H., A.P., and M.J. Critical revision of the manuscript for important intellectual content:  
320 S.-C.H., A.P., M.J., M.P.L., S.Y. and A.S.C. Supervision: S.Y. and A.S.C.

### 321 Acknowledgement

322 Research reported in this publication was supported by NIH grants R01 AR077604, R01 EB002524, R01  
323 AR079431, R01 HL155410, R01 LM012966, and P41 EB027060; NIH contracts 75N92020C00008 and  
324 75N92020C00021. The content is solely the responsibility of the authors and does not necessarily represent  
325 the official views of the National Institutes of Health

### 326 Competing interests

327 The authors declare no competing interests.

### 328 References

- 329 1. Hong, A. S. *et al.* Trends in Diagnostic Imaging Utilization among Medicare and Commercially  
330 Insured Adults from 2003 through 2016. *Radiology* **294**, 342–350 (2020).
- 331 2. Smith-Bindman, R. *et al.* Trends in Use of Medical Imaging in US Health Care Systems and in  
332 Ontario, Canada, 2000-2016. *JAMA* **322**, 843–856 (2019).
- 333 3. McDonald, R. J. *et al.* The effects of changes in utilization and technological advancements of cross-  
334 sectional imaging on radiologist workload. *Acad. Radiol.* **22**, 1191–1198 (2015).
- 335 4. Hosny, A., Parmar, C., Quackenbush, J., Schwartz, L. H. & Aerts, H. J. W. L. Artificial intelligence  
336 in radiology. *Nat. Rev. Cancer* **18**, 500–510 (2018).
- 337 5. Dan Lantsman, C. *et al.* Trend in radiologist workload compared to number of admissions in the

- 338 emergency department. *Eur. J. Radiol.* **149**, 110195 (2022).
- 339 6. Alonso-Martínez, J. L., Sánchez, F. J. A. & Echezarreta, M. A. U. Delay and misdiagnosis in sub-  
340 massive and non-massive acute pulmonary embolism. *Eur. J. Intern. Med.* **21**, 278–282 (2010).
- 341 7. Hendriksen, J. M. T. *et al.* Clinical characteristics associated with diagnostic delay of pulmonary  
342 embolism in primary care: a retrospective observational study. *BMJ Open* **7**, e012789 (2017).
- 343 8. Dunnmon, J. A. *et al.* Assessment of Convolutional Neural Networks for Automated Classification  
344 of Chest Radiographs. *Radiology* **290**, 537–544 (2019).
- 345 9. Rajpurkar, P. *et al.* Deep learning for chest radiograph diagnosis: A retrospective comparison of the  
346 CheXNeXt algorithm to practicing radiologists. *PLoS Med.* **15**, e1002686 (2018).
- 347 10. Larson, D. B. *et al.* Performance of a Deep-Learning Neural Network Model in Assessing Skeletal  
348 Maturity on Pediatric Hand Radiographs. *Radiology* **287**, 313–322 (2018).
- 349 11. Park, A. *et al.* Deep Learning–Assisted Diagnosis of Cerebral Aneurysms Using the HeadXNet  
350 Model. *JAMA Netw Open* **2**, e195600–e195600 (2019).
- 351 12. Bien, N. *et al.* Deep-learning-assisted diagnosis for knee magnetic resonance imaging: Development  
352 and retrospective validation of MRNet. *PLoS Med.* **15**, e1002699 (2018).
- 353 13. Esteva, A. *et al.* Prostate cancer therapy personalization via multi-modal deep learning on  
354 randomized phase III clinical trials. *NPJ Digit Med* **5**, 71 (2022).
- 355 14. Esteva, A. *et al.* Development and validation of a prognostic AI biomarker using multi-modal deep  
356 learning with digital histopathology in localized prostate cancer on NRG Oncology phase III clinical  
357 trials. *J. Clin. Orthod.* **40**, 222–222 (2022).
- 358 15. Esteva, A. *et al.* Dermatologist-level classification of skin cancer with deep neural networks. *Nature*  
359 **542**, 115–118 (2017).
- 360 16. Zech, J. R. *et al.* Variable generalization performance of a deep learning model to detect pneumonia  
361 in chest radiographs: A cross-sectional study. *PLoS Med.* **15**, e1002683 (2018).
- 362 17. LeCun, Y. & Misra, I. Self-supervised Learning: The Dark Matter of Intelligence. Preprint at (2021).
- 363 18. Devlin, J., Chang, M.-W., Lee, K. & Toutanova, K. BERT: Pre-training of Deep Bidirectional

- 364           Transformers for Language Understanding. *arXiv [cs.CL]* (2018).
- 365   19. Brown, Mann & Ryder. Language models are few-shot learners. *Adv. Neural Inf. Process. Syst.*
- 366   20. Chen, T., Kornblith, S., Norouzi, M. & Hinton, G. A Simple Framework for Contrastive Learning of
- 367           Visual Representations. *arXiv [cs.LG]* (2020).
- 368   21. Krishnan, R., Rajpurkar, P. & Topol, E. J. Self-supervised learning in medicine and healthcare. *Nat*
- 369           *Biomed Eng* (2022) doi:10.1038/s41551-022-00914-1.
- 370   22. Shurrab, S. & Duwairi, R. Self-supervised learning methods and applications in medical imaging
- 371           analysis: a survey. *PeerJ Comput Sci* **8**, e1045 (2022).
- 372   23. Lilian Weng, J. W. K. Self-Supervised Learning: Self-Prediction and Contrastive Learning. (2021).
- 373   24. Gidaris, S., Singh, P. & Komodakis, N. Unsupervised Representation Learning by Predicting Image
- 374           Rotations. *arXiv [cs.CV]* (2018).
- 375   25. Noroozi, M. & Favaro, P. Unsupervised Learning of Visual Representations by Solving Jigsaw
- 376           Puzzles. *arXiv [cs.CV]* (2016).
- 377   26. Doersch, C., Gupta, A. & Efros, A. A. Unsupervised Visual Representation Learning by Context
- 378           Prediction. *2015 IEEE International Conference on Computer Vision (ICCV)* Preprint at
- 379           <https://doi.org/10.1109/iccv.2015.167> (2015).
- 380   27. Schmidhuber, J. Deep learning in neural networks: an overview. *Neural Netw.* **61**, 85–117 (2015).
- 381   28. Kingma, D. P. & Welling, M. Auto-Encoding Variational Bayes. *arXiv [stat.ML]* (2013).
- 382   29. Goodfellow, I. J. *et al.* Generative Adversarial Networks. *arXiv [stat.ML]* (2014).
- 383   30. Vincent, P., Larochelle, H., Bengio, Y. & Manzagol, P.-A. Extracting and composing robust features
- 384           with denoising autoencoders. in *Proceedings of the 25th international conference on Machine*
- 385           *learning* 1096–1103 (Association for Computing Machinery, 2008).
- 386   31. Donahue & Simonyan. Large scale adversarial representation learning. *Adv. Neural Inf. Process.*
- 387           *Syst.*
- 388   32. Donahue, J., Krähenbühl, P. & Darrell, T. Adversarial Feature Learning. *arXiv [cs.LG]* (2016).
- 389   33. He, K., Fan, H., Wu, Y., Xie, S. & Girshick, R. Momentum Contrast for Unsupervised Visual

- 390 Representation Learning. *arXiv [cs.CV]* (2019).
- 391 34. Caron, M. *et al.* Emerging Properties in Self-Supervised Vision Transformers. *arXiv [cs.CV]* (2021).
- 392 35. Grill, Strub, Alché & Tallec. Bootstrap your own latent-a new approach to self-supervised learning.  
393 *Adv. Neural Inf. Process. Syst.*
- 394 36. Chen, X. & He, K. Exploring Simple Siamese Representation Learning. *arXiv [cs.CV]* (2020).
- 395 37. Caron, M. *et al.* Unsupervised Learning of Visual Features by Contrasting Cluster Assignments.  
396 *arXiv [cs.CV]* (2020).
- 397 38. Asano, Y. M., Rupprecht, C. & Vedaldi, A. Self-labelling via simultaneous clustering and  
398 representation learning. *arXiv [cs.CV]* (2019).
- 399 39. Gidaris, S., Bursuc, A., Komodakis, N., Perez, P. & Cord, M. Learning Representations by  
400 Predicting Bags of Visual Words. *2020 IEEE/CVF Conference on Computer Vision and Pattern*  
401 *Recognition (CVPR)* Preprint at <https://doi.org/10.1109/cvpr42600.2020.00696> (2020).
- 402 40. Pathak, D., Krahenbuhl, P., Donahue, J., Darrell, T. & Efros, A. A. Context Encoders: Feature  
403 Learning by Inpainting. *arXiv [cs.CV]* (2016).
- 404 41. He, K. *et al.* Masked Autoencoders Are Scalable Vision Learners. *arXiv [cs.CV]* (2021).
- 405 42. Bao, H., Dong, L. & Wei, F. BEiT: BERT Pre-Training of Image Transformers. *arXiv [cs.CV]*  
406 (2021).
- 407 43. Cunningham, P. & Delany, S. J. k-Nearest Neighbour Classifiers - A Tutorial. *ACM Comput. Surv.*  
408 **54**, 1–25 (2021).
- 409 44. Bozorgtabar, B., Mahapatra, D., Vray, G. & Thiran, J.-P. SALAD: Self-supervised Aggregation  
410 Learning for Anomaly Detection on X-Rays. in *Medical Image Computing and Computer Assisted*  
411 *Intervention – MICCAI 2020* 468–478 (Springer International Publishing, 2020).
- 412 45. Hsieh, W.-T., Lefort-Besnard, J., Yang, H.-C., Kuo, L.-W. & Lee, C.-C. Behavior Score-Embedded  
413 Brain Encoder Network for Improved Classification of Alzheimer Disease Using Resting State  
414 fMRI. *Conf. Proc. IEEE Eng. Med. Biol. Soc.* **2020**, 5486–5489 (2020).
- 415 46. Jiao, J. *et al.* Self-Supervised Contrastive Video-Speech Representation Learning for Ultrasound. in

- 416 *Medical Image Computing and Computer Assisted Intervention – MICCAI 2020* 534–543 (Springer  
417 International Publishing, 2020).
- 418 47. Tian, Y. *et al.* Constrained Contrastive Distribution Learning for Unsupervised Anomaly Detection  
419 and Localisation in Medical Images. in *Medical Image Computing and Computer Assisted  
420 Intervention – MICCAI 2021* 128–140 (Springer International Publishing, 2021).
- 421 48. Haghghi, F., Taher, M. R. H., Zhou, Z., Gotway, M. B. & Liang, J. Transferable Visual Words:  
422 Exploiting the Semantics of Anatomical Patterns for Self-supervised Learning. *IEEE Trans. Med.  
423 Imaging* **PP**, (2021).
- 424 49. Cornelissen & Putten. Evaluating self-supervised learning methods for downstream classification of  
425 neoplasia in barrett’s esophagus. *on Image Processing ...*
- 426 50. Li, X. *et al.* Rotation-Oriented Collaborative Self-Supervised Learning for Retinal Disease  
427 Diagnosis. *IEEE Trans. Med. Imaging* **40**, 2284–2294 (2021).
- 428 51. Fedorov, A. *et al.* Tasting the cake: evaluating self-supervised generalization on out-of-distribution  
429 multimodal MRI data. in *RobustML Workshop ICLR 2021* (2021).
- 430 52. Ouyang, J. *et al.* Self-supervised Longitudinal Neighbourhood Embedding. in *Medical Image  
431 Computing and Computer Assisted Intervention – MICCAI 2021* 80–89 (Springer International  
432 Publishing, 2021).
- 433 53. Ke, J., Shen, Y., Liang, X. & Shen, D. Contrastive Learning Based Stain Normalization Across  
434 Multiple Tumor in Histopathology. in *Medical Image Computing and Computer Assisted  
435 Intervention – MICCAI 2021* 571–580 (Springer International Publishing, 2021).
- 436 54. Yang, P., Hong, Z., Yin, X., Zhu, C. & Jiang, R. Self-supervised Visual Representation Learning for  
437 Histopathological Images. in *Medical Image Computing and Computer Assisted Intervention –  
438 MICCAI 2021* 47–57 (Springer International Publishing, 2021).
- 439 55. Sowrirajan, H., Yang, J., Ng, A. Y. & Rajpurkar, P. MoCo-CXR: MoCo Pretraining Improves  
440 Representation and Transferability of Chest X-ray Models. in *Proceedings of Machine Learning  
441 Research* 143:727–743 (2021).

- 442 56. Zhou, H.-Y. *et al.* Comparing to Learn: Surpassing ImageNet Pretraining on Radiographs by  
443 Comparing Image Representations. in *Medical Image Computing and Computer Assisted*  
444 *Intervention – MICCAI 2020* 398–407 (Springer International Publishing, 2020).
- 445 57. Sun, L., Yu, K. & Batmanghelich, K. Context Matters: Graph-based Self-supervised Representation  
446 Learning for Medical Images. in *Proc Conf AAAI Artif Intell.* (2021).
- 447 58. Burlina, P. *et al.* Low-Shot Deep Learning of Diabetic Retinopathy With Potential Applications to  
448 Address Artificial Intelligence Bias in Retinal Diagnostics and Rare Ophthalmic Diseases. *JAMA*  
449 *Ophthalmol.* **138**, 1070–1077 (2020).
- 450 59. Li, X., Jia, M., Islam, M. T., Yu, L. & Xing, L. Self-Supervised Feature Learning via Exploiting  
451 Multi-Modal Data for Retinal Disease Diagnosis. *IEEE Trans. Med. Imaging* **39**, 4023–4033 (2020).
- 452 60. Fedorov, A. *et al.* On self-supervised multi-modal representation learning: An application to  
453 Alzheimer’s disease. in *IEEE 18th International Symposium on Biomedical Imaging* (2021).
- 454 61. Mojab, N. *et al.* Real-World Multi-Domain Data Applications for Generalizations to Clinical  
455 Settings. in *2020 19th IEEE International Conference on Machine Learning and Applications*  
456 *(ICMLA)* 677–684 (2020).
- 457 62. Li, B., Li, Y. & Eliceiri, K. W. Dual-stream Multiple Instance Learning Network for Whole Slide  
458 Image Classification with Self-supervised Contrastive Learning. in *Proceedings of the IEEE/CVF*  
459 *conference on computer vision and pattern recognition.* (2021).
- 460 63. Dehaene, O., Camara, A., Moindrot, O., de Lavergne, A. & Courtiol, P. Self-Supervision Closes the  
461 Gap Between Weak and Strong Supervision in Histology. in *ML4H 2020 NeurIPS workshop* (2020).
- 462 64. Ciga, O., Xu, T. & Martel, A. L. Self supervised contrastive learning for digital histopathology.  
463 *Machine Learning with Applications* **7**, (2022).
- 464 65. Reed, C. J. *et al.* Self-Supervised Pretraining Improves Self-Supervised Pretraining. in *Proceedings*  
465 *of the IEEE/CVF Winter Conference on Applications of Computer Vision* (2022).
- 466 66. Liu, F. *et al.* Self-supervised Mean Teacher for Semi-supervised Chest X-Ray Classification. in  
467 *Machine Learning in Medical Imaging* 426–436 (Springer International Publishing, 2021).

- 468 67. Hao, H., Didari, S., Woo, J. O., Moon, H. & Bangert, P. Highly Efficient Representation and Active  
469 Learning Framework for Imbalanced Data and its Application to COVID-19 X-Ray Classification.  
470 *Conference on Neural Information Processing Systems (NeurIPS 2021)* (2021).
- 471 68. Li, J. *et al.* Multi-task contrastive learning for automatic CT and X-ray diagnosis of COVID-19.  
472 *Pattern Recognit.* **114**, 107848 (2021).
- 473 69. Gazda, M., Gazda, J., Plavka, J. & Drotar, P. Self-supervised deep convolutional neural network for  
474 chest X-ray classification. *arXiv [eess.IV]* (2021).
- 475 70. Dong, N. & Voiculescu, I. Federated Contrastive Learning for Decentralized Unlabeled Medical  
476 Images. in *Medical Image Computing and Computer Assisted Intervention – MICCAI 2021* 378–387  
477 (Springer International Publishing, 2021).
- 478 71. Nguyen, N.-Q. & Le, T.-S. A Semi-Supervised Learning Method to Remedy the Lack of Labeled  
479 Data. in *2021 15th International Conference on Advanced Computing and Applications (ACOMP)*  
480 78–84 (2021).
- 481 72. Azizi, Mustafa, Ryan & Beaver. Big self-supervised models advance medical image classification.  
482 *Proc. Estonian Acad. Sci. Biol. Ecol.*
- 483 73. Truong, T., Mohammadi, S. & Lenga, M. How Transferable are Self-supervised Features in Medical  
484 Image Classification Tasks? in *Proceedings of Machine Learning for Health* (eds. Roy, S. *et al.*) vol.  
485 158 54–74 (PMLR, 2021).
- 486 74. Zhao, X. & Zhou, S. Fast Mixing of Hard Negative Samples for Contrastive Learning and Use for  
487 COVID-19. in *2021 4th International Conference on Big Data Technologies* 6–12 (Association for  
488 Computing Machinery, 2021).
- 489 75. Vu, Y. N. T. *et al.* MedAug: Contrastive learning leveraging patient metadata improves  
490 representations for chest X-ray interpretation. in *Proceedings of Machine Learning Research* 126:1–  
491 14 (2021).
- 492 76. Ji, Z. *et al.* Improving Joint Learning of Chest X-Ray and Radiology Report by Word Region  
493 Alignment. in *Machine Learning in Medical Imaging* 110–119 (Springer International Publishing,

- 494 2021).
- 495 77. Dong, H. *et al.* Case Discrimination: Self-supervised Feature Learning for the Classification of Focal  
496 Liver Lesions. in *Innovation in Medicine and Healthcare* 241–249 (Springer Singapore, 2021).
- 497 78. Islam, N. U., Gehlot, S., Zhou, Z., Gotway, M. B. & Liang, J. Seeking an Optimal Approach for  
498 Computer-Aided Pulmonary Embolism Detection. *Mach Learn Med Imaging* **12966**, 692–702  
499 (2021).
- 500 79. Bao, W., Jin, Y., Huang, C. & Peng, W. CT Image Classification of Invasive Depth of Gastric  
501 Cancer based on 3D-DPN Structure. in *The 11th International Workshop on Computer Science and*  
502 *Engineering (WCSE 2021)* 115–121.
- 503 80. Jian, G.-Z., Lin, G.-S., Wang, C.-M. & Yan, S.-L. Helicobacter Pylori Infection Classification Based  
504 on Convolutional Neural Network and Self-Supervised Learning. in *2021 the 5th International*  
505 *Conference on Graphics and Signal Processing* 60–64 (Association for Computing Machinery,  
506 2021).
- 507 81. Kaku, A., Upadhyay, S. & Razavian, N. Intermediate layers matter in momentum contrastive self  
508 supervised learning. in *35th Conference on Neural Information Processing Systems (NeurIPS 2021)*.  
509 (2021).
- 510 82. Yellapragada, B., Hornauer, S., Snyder, K., Yu, S. & Yiu, G. Self-Supervised Feature Learning and  
511 Phenotyping for Assessing Age-Related Macular Degeneration Using Retinal Fundus Images.  
512 *Ophthalmol Retina* **6**, 116–129 (2022).
- 513 83. Perek, S., Amit, M. & Hexter, E. Self Supervised Contrastive Learning on Multiple Breast  
514 Modalities Boosts Classification Performance. in *Predictive Intelligence in Medicine* 117–127  
515 (Springer International Publishing, 2021).
- 516 84. Dufumier, B. *et al.* Contrastive Learning with Continuous Proxy Meta-data for 3D MRI  
517 Classification. in *Medical Image Computing and Computer Assisted Intervention – MICCAI 2021*  
518 58–68 (Springer International Publishing, 2021).
- 519 85. Li, H. *et al.* Imbalance-Aware Self-supervised Learning for 3D Radiomic Representations. in



- 520 *Medical Image Computing and Computer Assisted Intervention – MICCAI 2021* 36–46 (Springer  
521 International Publishing, 2021).
- 522 86. Manna, S., Bhattacharya, S. & Pal, U. Interpretive self-supervised pre-training: boosting  
523 performance on visual medical data. in *Proceedings of the Twelfth Indian Conference on Computer  
524 Vision, Graphics and Image Processing* 1–9 (Association for Computing Machinery, 2021).
- 525 87. Roychowdhury, S., Tang, K. S., Ashok, M. & Sanka, A. SISE-PC: Semi-supervised Image  
526 Subsampling for Explainable Pathology Classification. in *2021 43rd Annual International  
527 Conference of the IEEE Engineering in Medicine Biology Society (EMBC)* 2806–2809 (2021).
- 528 88. Ren, Z., Guo, Y., Yu, S. X. & Whitney, D. Improve Image-based Skin Cancer Diagnosis with  
529 Generative Self-Supervised Learning. in *2021 IEEE/ACM Conference on Connected Health:  
530 Applications, Systems and Engineering Technologies (CHASE)* 23–34 (2021).
- 531 89. Zhao, Z. & Yang, G. Unsupervised Contrastive Learning of Radiomics and Deep Features for Label-  
532 Efficient Tumor Classification. in *Medical Image Computing and Computer Assisted Intervention –  
533 MICCAI 2021* 252–261 (Springer International Publishing, 2021).
- 534 90. Saillard, C. *et al.* Self supervised learning improves dMMR/MSI detection from histology slides  
535 across multiple cancers. *COMPAY@MICCAI* (2021).
- 536 91. Li, J., Lin, T. & Xu, Y. SSLP: Spatial Guided Self-supervised Learning on Pathological Images. in  
537 *Medical Image Computing and Computer Assisted Intervention – MICCAI 2021* 3–12 (Springer  
538 International Publishing, 2021).
- 539 92. Liu, Q. *et al.* SimTriplet: Simple Triplet Representation Learning with a Single GPU. in *Medical  
540 Image Computing and Computer Assisted Intervention – MICCAI 2021* 102–112 (Springer  
541 International Publishing, 2021).
- 542 93. Wang, X. *et al.* TransPath: Transformer-Based Self-supervised Learning for Histopathological  
543 Image Classification. in *Medical Image Computing and Computer Assisted Intervention – MICCAI  
544 2021* 186–195 (Springer International Publishing, 2021).
- 545 94. Sharmay, Y., Ehsany, L., Syed, S. & Brown, D. E. HistoTransfer: Understanding Transfer Learning

- 546 for Histopathology. in *2021 IEEE EMBS International Conference on Biomedical and Health*  
547 *Informatics (BHI)* 1–4 (2021).
- 548 95. Spahr, A., Bozorgtabar, B. & Thiran, J.-P. Self-Taught Semi-Supervised Anomaly Detection On  
549 Upper Limb X-Rays. in *2021 IEEE 18th International Symposium on Biomedical Imaging (ISBI)*  
550 1632–1636 (2021).
- 551 96. Li, G., Togo, R., Ogawa, T. & Haseyama, M. Triplet Self-Supervised Learning for Gastritis  
552 Detection with Scarce Annotations. in *2021 IEEE 10th Global Conference on Consumer Electronics*  
553 *(GCCE)* 787–788 (2021).
- 554 97. Hossain, M. B., Iqbal, S. M. H. S., Islam, M. M., Akhtar, M. N. & Sarker, I. H. Transfer learning  
555 with fine-tuned deep CNN ResNet50 model for classifying COVID-19 from chest X-ray images.  
556 *Inform Med Unlocked* **30**, 100916 (2022).
- 557 98. Osin, J. *et al.* Learning Personal Representations from fMRI by Predicting Neurofeedback  
558 Performance. in *Medical Image Computing and Computer Assisted Intervention – MICCAI 2020*  
559 469–478 (Springer International Publishing, 2020).
- 560 99. Zhao, Q., Liu, Z., Adeli, E. & Pohl, K. M. Longitudinal Self-Supervised Learning. *Med. Image Anal.*  
561 **71**, (2021).
- 562 100. Gamper, J. & Rajpoot, N. Multiple Instance Captioning: Learning Representations from  
563 Histopathology Textbooks and Articles. in *2021 IEEE/CVF Conference on Computer Vision and*  
564 *Pattern Recognition (CVPR)* 16544–16554 (2021).
- 565 101. Rivail, A. *et al.* Modeling Disease Progression in Retinal OCTs with Longitudinal Self-supervised  
566 Learning. in *Predictive Intelligence in Medicine* 44–52 (Springer International Publishing, 2019).
- 567 102. Droste, R. *et al.* Ultrasound Image Representation Learning by Modeling Sonographer Visual  
568 Attention. in *International conference on information processing in medical imaging 2019* (2019).
- 569 103. Ewen, N. & Khan, N. Targeted Self Supervision For Classification On A Small Covid-19 Ct Scan  
570 Dataset. in *2021 IEEE 18th International Symposium on Biomedical Imaging (ISBI)* 1481–1485  
571 (2021).

- 572 104. Manna, S., Bhattacharya, S. & Pal, U. Self-Supervised Representation Learning for Detection of  
573 ACL Tear Injury in Knee MR Videos. *Pattern Recognit. Lett.* **154**, 37–43 (2022).
- 574 105. Jiao, J., Droste, R., Drukker, L., Papageorghiou, A. T. & Alison Noble, J. Self-supervised  
575 Representation Learning for Ultrasound Video. in *2020 IEEE 17th International Symposium on*  
576 *Biomedical Imaging (ISBI)* (2020).
- 577 106. Abbas, A., Abdelsamea, M. M. & Gaber, M. M. 4S-DT: Self-Supervised Super Sample  
578 Decomposition for Transfer Learning With Application to COVID-19 Detection. *IEEE Trans Neural*  
579 *Netw Learn Syst* **32**, 2798–2808 (2021).
- 580 107. Vats, A., Pedersen, M. & Mohammed, A. A Preliminary Analysis of Self-Supervision for Wireless  
581 Capsule Endoscopy. in *2021 9th European Workshop on Visual Information Processing (EUVIP)* 1–  
582 6 (2021).
- 583 108. Ewen, N. & Khan, N. Online Unsupervised Learning For Domain Shift In Covid-19 CT Scan  
584 Datasets. in *2021 IEEE International Conference on Autonomous Systems (ICAS)* 1–5 (2021).
- 585 109. Zhu, Y. Self-supervised Learning for Small Shot COVID-19 Classification. in *2021 3rd*  
586 *International Conference on Information Technology and Computer Communications* 36–40  
587 (Association for Computing Machinery, 2021).
- 588 110. Long, Y. Pneumonia Identification with Self-supervised Learning and Transfer Learning. in  
589 *Application of Intelligent Systems in Multi-modal Information Analytics* 627–635 (Springer  
590 International Publishing, 2021).
- 591 111. Dezaki, F. T. *et al.* Echo-Rhythm Net: Semi-Supervised Learning For Automatic Detection of Atrial  
592 Fibrillation in Echocardiography. in *2021 IEEE 18th International Symposium on Biomedical*  
593 *Imaging (ISBI)* 110–113 (2021).
- 594 112. Wicaksono, R. S. H., Septiandri, A. A. & Jamal, A. Human Embryo Classification Using Self-  
595 Supervised Learning. in *2021 2nd International Conference on Artificial Intelligence and Data*  
596 *Sciences (AiDAS)* 1–5 (2021).
- 597 113. Vu, Y. N. T., Tsue, T., Su, J. & Singh, S. An improved mammography malignancy model with self-

598 supervised learning. in *Medical Imaging 2021: Computer-Aided Diagnosis* vol. 11597 210–216  
599 (SPIE, 2021).

600 114. Hashimoto, Y., Ogata, Y., Honda, M. & Yamashita, Y. Deep Feature Extraction for Resting-State  
601 Functional MRI by Self-Supervised Learning and Application to Schizophrenia Diagnosis. *Front.*  
602 *Neurosci.* **15**, 696853 (2021).

603 115. Srinidhi, C. L., Kim, S. W., Chen, F.-D. & Martel, A. L. Self-supervised driven consistency training  
604 for annotation efficient histopathology image analysis. *Med. Image Anal.* **75**, (2021).

605 116. Tamkin, A. *et al.* DABS: A Domain-Agnostic Benchmark for Self-Supervised Learning. in *NeurIPS*  
606 *2021 Datasets and Benchmarks Track* (2021).

607 117. Park, J., Kwak, I.-Y. & Lim, C. A Deep Learning Model with Self-Supervised Learning and  
608 Attention Mechanism for COVID-19 Diagnosis Using Chest X-ray Images. *Electronics* **10**, 1996  
609 (2021).

610 118. Jana, A. *et al.* Liver Fibrosis And NAS Scoring From CT Images Using Self-Supervised Learning  
611 And Texture Encoding. in *2021 IEEE 18th International Symposium on Biomedical Imaging (ISBI)*  
612 1553–1557 (2021).

613 119. Zhong, H. *et al.* A Self-supervised Learning Based Framework for Automatic Heart Failure  
614 Classification on Cine Cardiac Magnetic Resonance Image. in *2021 43rd Annual International*  
615 *Conference of the IEEE Engineering in Medicine Biology Society (EMBC)* 2887–2890 (2021).

616 120. Jung, W., Heo, D.-W., Jeon, E., Lee, J. & Suk, H.-I. Inter-regional High-Level Relation Learning  
617 from Functional Connectivity via Self-supervision. in *Medical Image Computing and Computer*  
618 *Assisted Intervention – MICCAI 2021* 284–293 (Springer International Publishing, 2021).

619 121. Liu, C. *et al.* TN-USMA Net: Triple normalization-based gastrointestinal stromal tumors  
620 classification on multicenter EUS images with ultrasound-specific pretraining and meta attention.  
621 *Med. Phys.* **48**, 7199–7214 (2021).

622 122. Tian, Y. *et al.* Constrained Contrastive Distribution Learning for Unsupervised Anomaly Detection  
623 and Localisation in Medical Images. *arXiv [cs.CV]* (2021).

- 624 123. Irvin, J. *et al.* CheXpert: A Large Chest Radiograph Dataset with Uncertainty Labels and Expert  
625 Comparison. *arXiv [cs.CV]* (2019).
- 626 124. Colak, E. *et al.* The RSNA Pulmonary Embolism CT Dataset. *Radiol Artif Intell* **3**, e200254 (2021).
- 627 125. Zhou, Y. *et al.* RadFusion: Benchmarking Performance and Fairness for Multimodal Pulmonary  
628 Embolism Detection from CT and EHR. *arXiv [eess.IV]* (2021).
- 629 126. Johnson, A. E. W. *et al.* MIMIC-CXR-JPG, a large publicly available database of labeled chest  
630 radiographs. *arXiv [cs.CV]* (2019).
- 631 127. Zhang, S., Zou, B., Xu, B., Su, J. & Hu, H. An Efficient Deep Learning Framework of COVID-19  
632 CT Scans Using Contrastive Learning and Ensemble Strategy. in *2021 IEEE International  
633 Conference on Progress in Informatics and Computing (PIC)* 388–396 (2021).
- 634 128. Liu, Q. *et al.* SimTriplet: Simple Triplet Representation Learning with a Single GPU. *arXiv [cs.CV]*  
635 (2021).
- 636 129. Hellerhoff. File:Kavernom rechts parietal 59M - MR - 001.jpg. *Wikimedia*  
637 [https://commons.wikimedia.org/wiki/File:Kavernom\\_rechts\\_parietal\\_59M\\_-\\_MR\\_-\\_001.jpg](https://commons.wikimedia.org/wiki/File:Kavernom_rechts_parietal_59M_-_MR_-_001.jpg) (2022).
- 638 130. Matio, H. File:Dog Breeds.jpg. *Wikimedia Commons*  
639 [https://commons.wikimedia.org/wiki/File:Dog\\_Breeds.jpg](https://commons.wikimedia.org/wiki/File:Dog_Breeds.jpg) (2019).
- 640 131. Kotar, Ilharco & Schmidt. Contrasting contrastive self-supervised representation learning pipelines.  
641 *Proc. Estonian Acad. Sci. Biol. Ecol.*
- 642 132. Cole, E., Yang, X., Wilber, K., Aodha, O. M. & Belongie, S. When Does Contrastive Visual  
643 Representation Learning Work? *arXiv [cs.CV]* (2021).
- 644 133. Kolesnikov, A. *et al.* Big Transfer (BiT): General Visual Representation Learning. *arXiv [cs.CV]*  
645 (2019).
- 646 134. Azizi, S. *et al.* Robust and Efficient Medical Imaging with Self-Supervision. *arXiv [cs.CV]* (2022).
- 647 135. Yan, R. *et al.* Label-Efficient Self-Supervised Federated Learning for Tackling Data Heterogeneity  
648 in Medical Imaging. *arXiv [cs.CV]* (2022).
- 649 136. Shi, Y., Siddharth, N., Torr, P. H. S. & Kosiorek, A. R. Adversarial Masking for Self-Supervised

- 650 Learning. *arXiv [cs.CV]* (2022).
- 651 137. Li, G. *et al.* SemMAE: Semantic-Guided Masking for Learning Masked Autoencoders. *arXiv*  
652 *[cs.CV]* (2022).
- 653 138. Van Gansbeke & Vandenhende. Revisiting contrastive methods for unsupervised learning of visual  
654 representations. *Adv. Eng. Educ.*
- 655 139. Peng, Wang, Zhu & Wang. Crafting better contrastive views for siamese representation learning.  
656 *Proc. Estonian Acad. Sci. Biol. Ecol.*
- 657 140. Taleb, Kirchler & Monti. ConTIG: Self-supervised Multimodal Contrastive Learning for Medical  
658 Imaging with Genetics. *Proc. IEEE.*
- 659 141. Zhang, Y., Jiang, H., Miura, Y., Manning, C. D. & Langlotz, C. P. Contrastive Learning of Medical  
660 Visual Representations from Paired Images and Text. *arXiv [cs.CV]* (2020).
- 661 142. Huang, S.-C., Shen, L., Lungren, M. P. & Yeung, S. GLoRIA: A multimodal global-local  
662 representation learning framework for label-efficient medical image recognition. in *2021 IEEE/CVF*  
663 *International Conference on Computer Vision (ICCV)* (IEEE, 2021).  
664 doi:10.1109/iccv48922.2021.00391.
- 665 143. Russakovsky, O. *et al.* ImageNet Large Scale Visual Recognition Challenge. *Int. J. Comput. Vis.*  
666 **115**, 211–252 (2015).
- 667 144. Moher, D. *et al.* Preferred reporting items for systematic review and meta-analysis protocols  
668 (PRISMA-P) 2015 statement. *Syst. Rev.* **4**, 1 (2015).
- 669 145. Danu, M., Ciuşdel, C. F. & Itu, L. M. Deep learning models based on automatic labeling with  
670 application in echocardiography. in *2020 24th International Conference on System Theory, Control*  
671 *and Computing (ICSTCC)* 373–378 (2020).

672